

RESEARCH

Open Access



The role of functional imaging; DWI, ADC and ^{18}F -FDG PET/CT in the evaluation of HCC treatment response after transarterial chemoembolization

Ahmed S. Abdelrahman , Amgad S. Abdel-Rahman and Noha M. Taha

Abstract

Background: The transcatheter arterial chemoembolization (TACE) is one of the treatment lines for patients with hepatocellular carcinoma (HCC), this study was conducted to assess the role of functional imaging including the DWI, ADC and ^{18}F -2-fluoro-2-deoxyglucose (FDG) positron emission tomography-computed tomography (PET/CT) for detection of residual HCC after TACE as compared to the structural liver imaging reporting and data system (LI-RADS).

Results: The optimal cut off value of standardized uptake value ratio ($\text{SUV}_{\text{max}}/\text{liver SUV}_{\text{mean}}$ ratio) for detection of residual viable HCC after TACE was 1.09 with 88.9%, 87.5% and 88.6% sensitivity, specificity, and accuracy respectively, a lower diagnostic value was noted in the qualitative visual FDG PET/CT assessment with sensitivity, specificity, and accuracy of 81.5%, 75% and 80% respectively. The sensitivity, specificity, and accuracy of DWI for identification of post-TACE viable HCC were 77.8%, 75%, and 77.1% respectively. The optimal cut off value of ADC for the diagnosis of variable HCC was $1.32 \times 10^{-3} \text{ mm}^2/\text{s}$ with sensitivity, specificity, and accuracy of 81.5%, 75%, and 80% respectively.

Conclusions: DWI, ADC and FDG PET/CT are effective functional imaging modalities for the evaluation of viable residual HCC post-TACE with comparable findings for the dynamic cross-section imaging.

Keywords: HCC, TACE, LI-RADS PET, DWI

Background

Hepatocellular carcinoma (HCC) is one of the most common primary hepatic tumors, it has been ranked the fourth leading cause of cancer-related deaths in 2018, and the sixth most common malignancy worldwide [1, 2]. Liver cirrhosis and viral hepatitis are considered the major risk factors for the development of HCC [3].

Surgical resection of HCC, as well as liver transplantation, are the first and best lines for the treatment of patients with HCC [4]. However, only 20% of these patients can be treated surgically, because of the

associated comorbidity related to liver cirrhosis and the advanced stage of the tumors at the time of diagnosis [5], so the palliative treatment which includes transcatheter arterial chemoembolization (TACE), radiofrequency thermal ablation, immunotherapy, systemic chemotherapy, and local injection, is considered the next line of treatment for these patients [6]. TACE is the treatment of choice for patients with intermediate-stage HCC and patients with large or multicentric HCC [7]. Monitoring the treatment response after TACE with imaging is an essential step for determining the outcome of TACE and the next further phase in the patient management plan [3].

Triphasic contrast-enhanced computerized tomography (CECT) was considered the standard imaging

*Correspondence: dr_ahmedsamy@yahoo.com
Radiology Department, Faculty of Medicine, Ain Shams University, Cairo, Egypt

technique for the diagnosis of HCC and for assessing HCC post-TACE. Beam hardening artefact related to retained hyper-dense lipiodol material may interfere with the proper detection of contrast enhancement within a viable tumor and interfere with the ability of CECT to detect the residual tumor after TACE [4]. Dynamic contrast-enhanced magnetic resonance imaging (DCE-MRI) is a well-established modality in the imaging of liver and hepatic focal lesions, MRI signal wasn't degraded by lipiodol droplets; thus, the newly formed/residual lesions are best identified by the DCE-MRI [3, 8]. The liver imaging reporting and data system (LI-RADS) has released an algorithm for evaluating the treatment response of HCC after locoregional therapy which depend mainly upon the enhancement features in the dynamic contrast enhancement study [9].

Recently, positron emission tomography (PET) with ^{18}F -2-fluoro-2-deoxyglucose (FDG) has emerged and used for baseline staging and monitoring the treatment response in different tumors. FDG PET/CT detects the glucose metabolism of the tumors, providing unique information that cannot be detected from other conventional imaging techniques, and allows whole-body imaging and surveillance [10]. The diagnostic accuracy of FDG PET/CT for diagnosis of HCC is still controversial, especially in the well-differentiated HCC [11, 12], yet later reports have described the favorable diagnostic performance of FDG PET in detecting metastatic and recurrent HCC [13, 14].

Diffusion-weighted image (DWI) provides an idea of the movement of the intracellular and extracellular water molecule in the biological tissue and thus gives data on the microenvironment of the tumor [1, 15]. DWI and apparent diffusion coefficient (ADC) provide qualitative and quantitative information about tissue viability. The viable tumoral tissue exhibited restricted diffusion with relatively low ADC, while necrotic post-treatment tumor has increased water facilitation and increased ADC value [16].

The aim of this study was to emphasize the role of functional imaging of the DWI, ADC and the FDG PET/CT in early detection of post-TACE residual/recent HCC compared to the liver imaging reporting and data system (LI-RADS).

Methods

Patients

Thirty-five patients with a mean age of 59.1 ± 5.8 years were retrospectively evaluated after approval of our ethical committee which waived the requirement for written consent. The images were retrieved from the picture archiving and communication system. During the period of August 2019 and January 2021, all TACE-treated

HCC patients who were treated with iodized oil, with the three-month post-treatment DWI, ADC, FDG PET/CT, triphasic CECT and DCE-MRI imaging surveillance were interpreted according to the LI-RADS v2018 treatment response design were included in our research. The exclusion criteria incorporated patients with missed one of the dynamic contrast studies, DWI with ADC or FDG PET/CT, HCC lesion with equivocally viable treatment response LI-RADS score, and poor-quality images which hinder proper assessment of treatment response.

Technique of DCE MRI examination

- The MRI examination was done using 1.5 T MRI (Philips Achieva scanner, Healthcare, Netherlands) with an eight-channel phased-array coil. A respiratory belt was paced around the patient abdomen for synchronization of the patient breath. Field of view: $33 \times 27 \times 22$ cm. Matrix: 256×224 . Slice thickness 8 mm, gap: 0.7 mm. Sequences: Axial T2 WI single shot spine echo (TR/TE: 7300/115 ms), Breath-hold coronal single-shot T2-WI turbo spin-echo (TSE) (TR/TE: 704/310 ms, 90° flip angle). In phase axial T1-weighted gradient echo (TR/TE: 10/4.5 ms), Out of phase axial T1-weighted gradient echo (TR/TE: 10/2.2 ms, 15° flip angle) Respiratory-triggered axial DWI (echo-planar imaging (EPI); b values, 0, 200 and 800 s/mm^2 ; TR/TE: 2300/63 ms, 80 EPI factor, 5 mm slice thickness, 1 mm gap, 90° flip angle, 2 acceleration factor). Post-processed ADC map was generated, and ADC values were then calculated. Dynamic multiphase T1-weighted high-resolution isotropic volume examination (THRIVE), a spoiled 3 D gradient fat-suppressed sequence (TR/TE: 3.8/1.8 ms, 12° flip angle, and slice thickness: 2–3 mm) that included T1 pre-contrast, late arterial phase (20–30 s), portal/venous phase (60–90 s), and delayed phases (180–210 s), was performed after the injection of 10–20 ml gadolinium contrast media at a rate of 2 ml/s.

Technique of FDG PET/CT technique examination

- Hybrid PET and CT images were performed using PET/CT system (GE medical system; Discovery IQ 16 PET/CT scanner; USA). The whole-body PET images from the skull vault down to the knee was performed using several bed positions acquisition, each bed was approximately 15 cm axial filed with 4 mm special resolution. The time of acquisition of the emission scan was about 2 min for each bed, with a total time range between 12 and 17 min. The patients were informed to fast 6–8 h before the examination and the blood glucose level was kept below 200 mg/

Table 1 Diagnostic performance of DWI, ADC, SUV ratio and functional imaging

	DWI	ADC*	PET	SUV ratio [†]
Viable	23	24	24	25
Non-viable	12	11	11	10
TP	21	22	22	24
TN	6	6	6	7
FP	2	2	2	1
FN	6	5	5	3
Sensitivity	77.8%	81.5%	81.5%	88.9%
Specificity	75%	75%	75%	87.5%
Accuracy	77.1%	80%	80%	88.6

TP true positive, TN true negative, FP false positive, FN false negative

*ADC cut off value ($1.32 \times 10^{-3} \text{ mm}^2/\text{s}$)

[†] SUV ratio (Tumor SUV_{max} /liver SUV_{mean} cut off value = 1.09)

dl before injecting the tracer. The scan was performed 45–60 min after injection of 0.1 mCi 18 F-FDG/kg.

- A diagnostic triphasic contrast-enhanced transmission scan was done immediately after PET images, after injection of 100 millilitres of non-ionic iodinated contrast media (omnipaque 300) at a rate of 2–3 ml/s. CT has been performed with the following parameters: 350 mA, 120 kV, 0.5 tube rotation time and 5 mm slice thickness. The arterial phase covering the region of the abdomen from the base of the lungs down to the iliac bones, the venous phase covering the same field of view as the PET images and the delayed phase covering from the skull bases down to the inferior pubic rami.
- GE workstation was used to review the PET, CT and the fused PET/CT images, multi-planner reformatted images, 3D maximum intensity projection images were reconstructed for the PET images.

Analysis of data

Imaging analysis

- The FDG PET/CT images were independently evaluated by two radiologists with 10 and 7 years of experience

in the nuclear medicine field, and in cases of discrepancy, a final diagnosis was reached by consensus.

- The FDG PET/CT images were first evaluated by the qualitative visual analysis which was considered as positive for viable HCC when an eccentric, nodular, or scattered FDG uptake was detected, yet if the FDG uptake was visually graded as equal to or lower than the surrounding liver parenchyma, the lesion was considered as non-viable well ablated HCC. A uniform FDG uptake or regular peripheral rim of uptake were also considered well-ablated HCC.
- The quantitative analysis of the FDG PET/CT examination was performed by measuring the standardized uptake value (SUV) by drawing a region of interest (ROI) in the tumor and hepatic parenchyma in the contralateral hepatic lobe. Tumor maximum SUV (SUV_{max}), and liver parenchyma mean SUV (SUV_{mean}) was measured, then the SUV ratio of tumor SUV_{max} to liver SUV_{mean} was calculated.
- The qualitative assessment of DWI was analyzed visually, and viable HCC was diagnosed if the lesion expressed a bright signal in the DWI with b value of $800 \text{ s}/\text{mm}^2$ with low signal in the corresponding ADC map, otherwise, the HCC was considered non-viable well ablated if these features were missed. The DWI and ADC map were reviewed in Philips IntelliSpace Portal Image and information management software V 9.0. (Philips Medical System Nederland B.V), where the quantitative analysis was performed by drawing a region of interest (ROI) in the most hypointense area of the ADC map to measure the ADC value.
- Dynamic contrast-enhanced images were considered the standard reference in the current study, and it was reported blindly and independently by experienced radiologists according to the American Association for the Study of Liver Diseases (AASLD) and LI-RADS v2018 lexicon [17, 18]: LR-TR nonviable for a non-enhancing lesion or expected treatment-specific enhancement pattern noted. LR-TR viable for residual nodular, mass-like, or thick irregular tissue within or along the treated HCC associated

Table 2 ADC, tumor SUV_{max} and SUV ratio of post TACE viable and nonviable HCC

	Viable HCC		Nonviable HCC		Value*	p value	Sig.
	Mean \pm SD	Range	Mean \pm SD	Range			
ADC ($\times 10^{-3} \text{ mm}^2/\text{s}$)	1.06 \pm 0.24	0.58–1.39	1.55 \pm 0.33	1.23–2.08	4.677	<0.001	S
Tumor SUV_{max}	4.26 \pm 0.15	2.4–7.9	2.46 \pm 1.05	1.1–3.9	–3.966	<0.001	S
SUV ratio	1.42 \pm 0.54	1–2.11	0.92 \pm 0.26	0.54–1.31	–3.028	0.005	S

S significant

*Independent sample t test

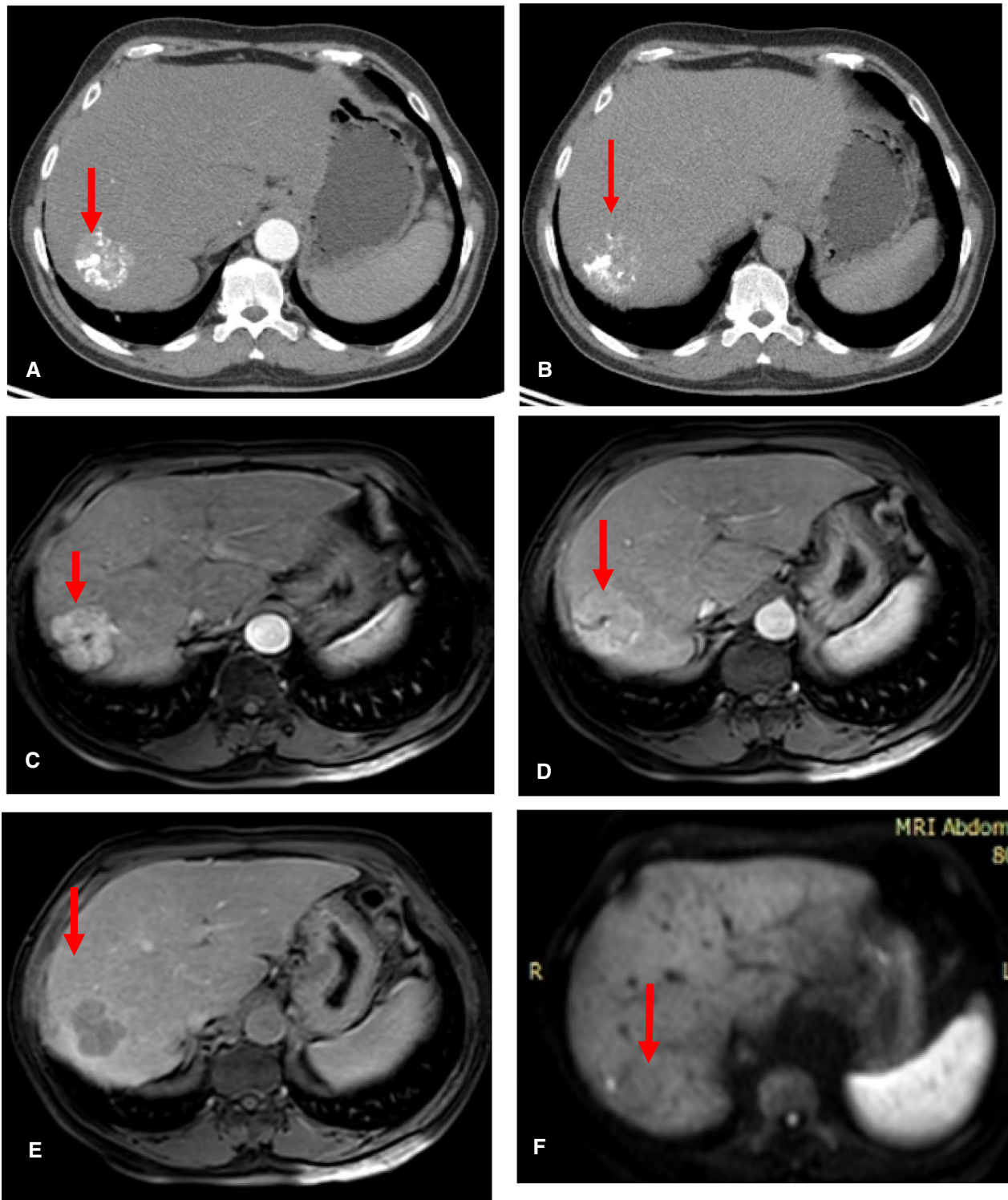


Fig. 1 63 years old male patient underwent TACE. PET/CT uptake with diffusion restriction in TR-LR viable lesion. **A, B** Axial arterial phase (**A**) and venous phase (**B**) CT images showing embolized lesion with heterogeneous lipiodol concentration, APHE and washout (red arrow). **C–E** Axial arterial (**C**), venous (**D**) and delayed (**E**) dynamic contrast MRI images also showing APHE, delayed washout and delayed capsular enhancement (TR-LR viable). **F–H** DWI (**F**) and ADC map (**G, H**), the lesion is iso-intense in the DWI with low ADC value compared to the adjacent liver, the mean ADC of the lesion is $1.12 \times 10^{-3} \text{ mm}^2/\text{s}$. **I–K** Axial PET/CT fused images showing increased FDG uptake in the residual lesion achieving SUV max of 2.59 while the mean SUV of the liver was 1.66 (SUV ratio is 1.56)

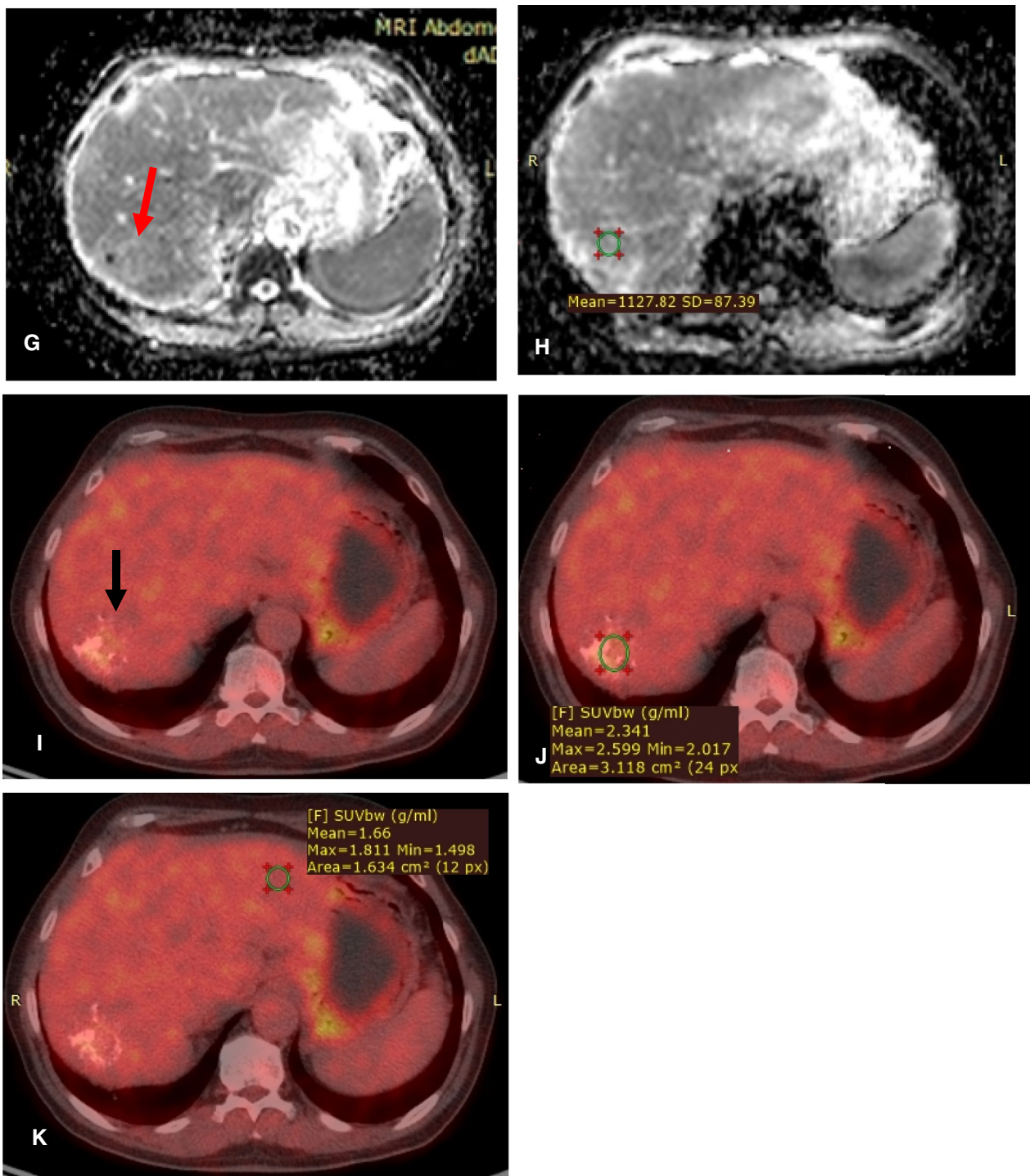


Fig. 1 continued

with one or more of the following features 1- arterial phase hyperenhancement, 2- washout appearance, 3- enhancement similar to pretreated HCC. The TR-LR equivocal and non-evaluable were excluded in the current study. The hemorrhage is identified by its typical signal in MRI images where it mostly displayed hyperintense signal in T1 WIs and is either hyperintense or hypointense in T2 WIs (depending on its stage). The pre-contrast T1 WI sequence, subtraction images and washout images were used to determine the contrast enhancement.

Statistical analysis

- Data were analyzed using Statistical Package for Social Science (IBM Corp. Released 2017. IBM SPSS Statistics for Windows, Version 25.0. Armonk, NY: IBM Corp.). Parametric quantitative data were expressed as mean \pm standard deviation (SD). Median and range were used to report the non-parametric quantitative data. Qualitative data were described as frequency and percentage. An independent same *t*-test was performed to compare the mean of continuous variables. The diagnostic performance of the categorical variable was performed using cross-tabulation. The sensitivity, specificity, and accuracy were then calculated. Receiver operator characteristic (ROC) curve analysis was performed to determine the optimal cut off value. Multinomial logistic regression models using enter method and forward method were reconstructed to specify the optimal predicting variable for viable HCC. The odd ratio reciprocal was calculated to describe the negative association as follow; odd ratio reciprocal = 1/original odd ratio. *p* value < 0.05 was considered statistically significant.

Results

Thirty-five patients with post-TACE HCC were examined with mean patient age of 59.1 ± 5.8 years (range 43 to 74 years), 20 (57.1%) patients were males and 15 (42.9%) were females.

The final diagnosis based upon LI-RADS v2018 revealed post-TACE LR-TR viable HCC in 27 patients; 6/27 (22.2%) revealed thick irregular enhancement pattern, and 21/27 (77.8%) revealed nodular and mass enhancement pattern, the mean size of the viable lesions was 3.4 ± 1.8 cm (range from 1.2 to 6.5 cm), yet the mean pretreatment size was 6.7 ± 1.6 cm (range from 3.5 to 8.9 cm). On the other hand, eight patients were diagnosed as LR-TR non-viable with a well-ablated HCC and pretreatment size mean of 4.9 ± 0.8 cm (range from 3.8 to 6.2 cm).

Diagnostic performance of qualitative FDG PET/CT and DWI

The visual assessment of the PET revealed residual viable HCC in 24 patients and non-viable HCC in 11 patients with sensitivity, specificity, and accuracy of 81.5%, 75% and 80% respectively. The qualitative DWI revealed 23 patients with restricted diffusion which were diagnosed as viable HCC, on the other hand, no diffusion restriction was noted in 12 patients which were diagnosed by the DWI as a non-viable well ablated HCC. The sensitivity, specificity, and accuracy of DWI were 77.8%, 75%, and 77.1% respectively (Table 1).

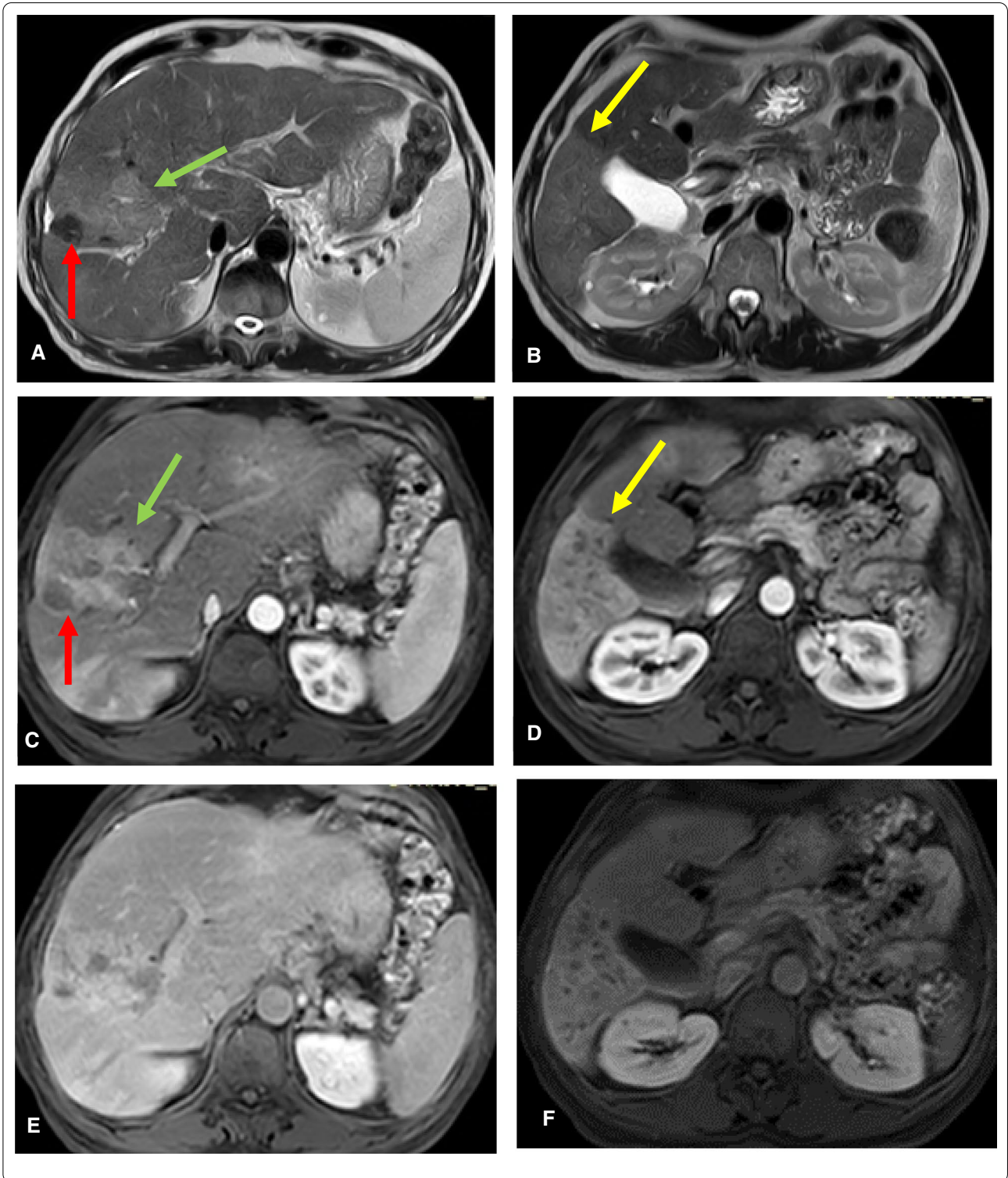
Diagnostic performance of quantitative SUV and ADC

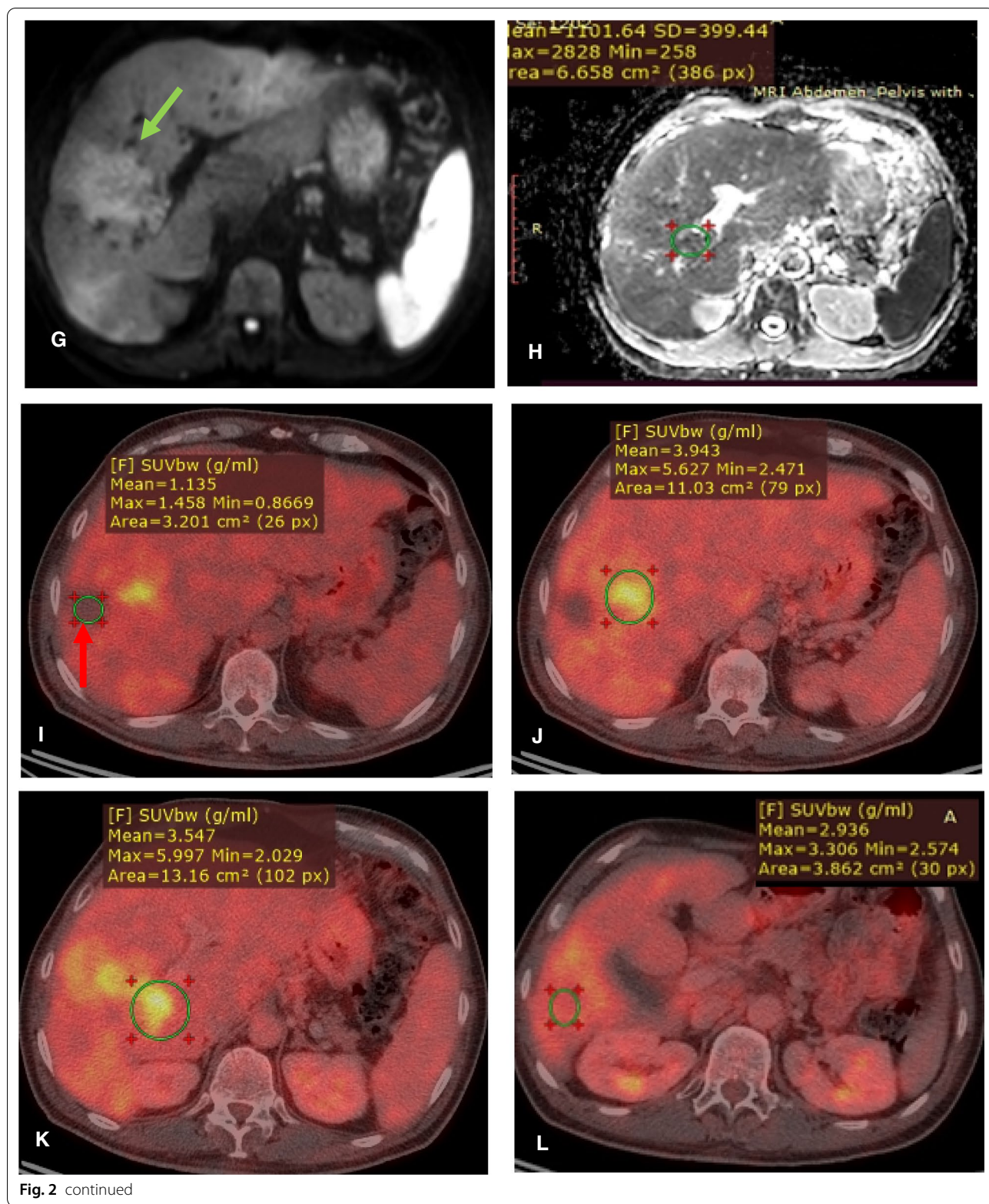
The quantitative assessment of the SUV revealed that the mean value of the SUV_{max} and SUV ratio (tumor SUV_{max} /liver SUV_{mean}) for the residual viable HCC was significantly higher than the non-viable treated HCC (*p* < 0.001 and 0.005 respectively), yet the mean ADC value of the viable HCC post-TACE was significantly lower than the non-viable HCC (*p* < 0.001) (Table 2).

The optimal cut off point of the SUV ratio was 1.09 (AUC = 0.926, 95% CI 0.822–1.000, *p* < 0.001) (Fig. 1), which revealed sensitivity, specificity, and accuracy of 88.9%, 87.5% and 88.6% respectively. On the other hand, the optimal ADC cut off value for discrimination between viable and non-viable HCC was 1.32×10^{-3} mm²/s (AUC = 0.889, 95% CI 0.777–1.000, *p* value < 0.001) (Figs. 2, 3), with sensitivity, specificity, and accuracy of 81.5%, 75%, and 80% respectively (Tables 1, 3; Figs. 4, 5).

(See figure on next page.)

Fig. 2 60 years old male patient underwent TACE. PET/CT uptake and diffusion restriction in TR-LR viable lesion with tumoral right portal vein thrombosis. **A, B** MRI T2 WI showing hypointense necrotic ablated lesion (red arrow) with medial hyperintense lesion (green arrow) and wedge-shaped hyperintense area in hepatic sub-segment VI (yellow arrow). **C–F** arterial (**C, D**), and delayed (**E, F**) DCE MRI showing the necrotic ablated non-enhancing area (red arrow), residual viable HCC (green arrow) which shows APHE and washout, the right portal vein branch is occluded with tumoral thrombus. A persistent enhancing subsegment VI wedge-shaped lesion in the arterial and delayed phase (yellow arrow) is seen and it corresponds to transient hepatic attenuation differences (THAD). **G, H** DWI (**G**) and ADC map (**H**) the lesion is hyperintense in the DWI with low ADC value compared to the adjacent liver, the mean ADC of the portal vein lesion is 1.1×10^{-3} mm²/s. **I–L** axial PET/CT fused images showing necrotic lesion with SUV max measuring 1.45 (**I**), residual non ablated HCC with increased FDG uptake (**J**) and involvement of the right portal vein branch (**K**), the SUV max measures 5.62 and 5.99 in the viable HCC and the tumoral portal vein lesion respectively. No focal uptake was seen in the hepatic sub-segment VI THAD area with SUV max measuring 3.3 (**L**)





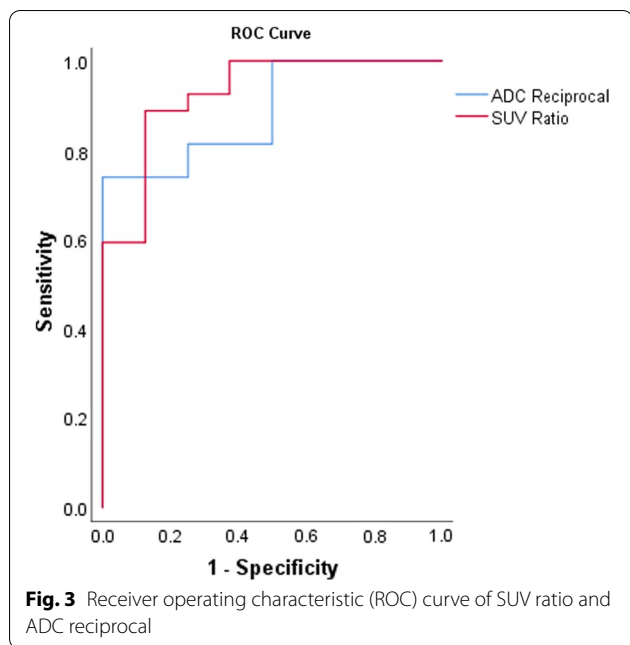


Table 3 Area under the curve of ADC and tumor ratio for detection of post-TACE viable HCC

	AUC	95% Confidence interval	p value	Sig.
ADC	0.889	0.777–1.000	<0.001	S
SUV ratio	0.926	0.822–1.000	<0.001	S

S significant

The PET/CT revealed extrahepatic metastatic lesions in three patients, one of them also suffered from de novo HCCs (Fig. 6).

Logistic regression analysis of DW, PET, ADC value and SUV ratio

Initially, each logistic regression was reconstructed using DWI, PET, ADC value, or SUV ratio variables separately, and all were significant (Table 4). DWI and PET were found to have a positive significant correlation with viable HCC ($B=2.351$ and 2.580 , respectively), with an odd ratio of 10.5 and 13.2 ($p=0.012$ and 0.007 , respectively). A negative significant association was found between the ADC value and the viable HCC ($B=-9.609$), the odd ratio for each point increase in the ADC value

(continuous variable) was 0.000067 ($p=0.036$), which indicated that with each 0.01 rise in the ADC value, the odd ratio for viable HCC decreased by 0.000067 , and in other words, for each 0.01 elevation in the ADC value, the odd ratio for non-viable HCC increases by 1492 . Finally, a significant positive correlation was discovered between the SUV ratio and viable HCC ($B=10.697$), the odd ratio for each point rise in the SUV ratio (continuous variable) was $44,219$ ($p=0.022$), which implied that the odd ratio for viable HCC increased by $44,219$ for every 0.01 increment in the SUV ratio.

Then, using the enter method, a multinomial logistic regression model was constructed by adding all variables, and the odd ratio for all variables in this model was insignificant (Table 5). Finally, a multinomial logistic regression model was reconstructed using the forward method, which specified the ADC value as the best variable for predicting viable HCC with an odd ratio of 0.000067 ($p=0.036$) (Table 6) and 88.6% model accuracy, the optimal ADC value for predicting viable HCC in this model was $1.35 \times 10^{-3} \text{ mm}^2/\text{s}$, according to the logistic equation [$13.479 + (\text{ADC value} \times -9.609)$].

Discussion

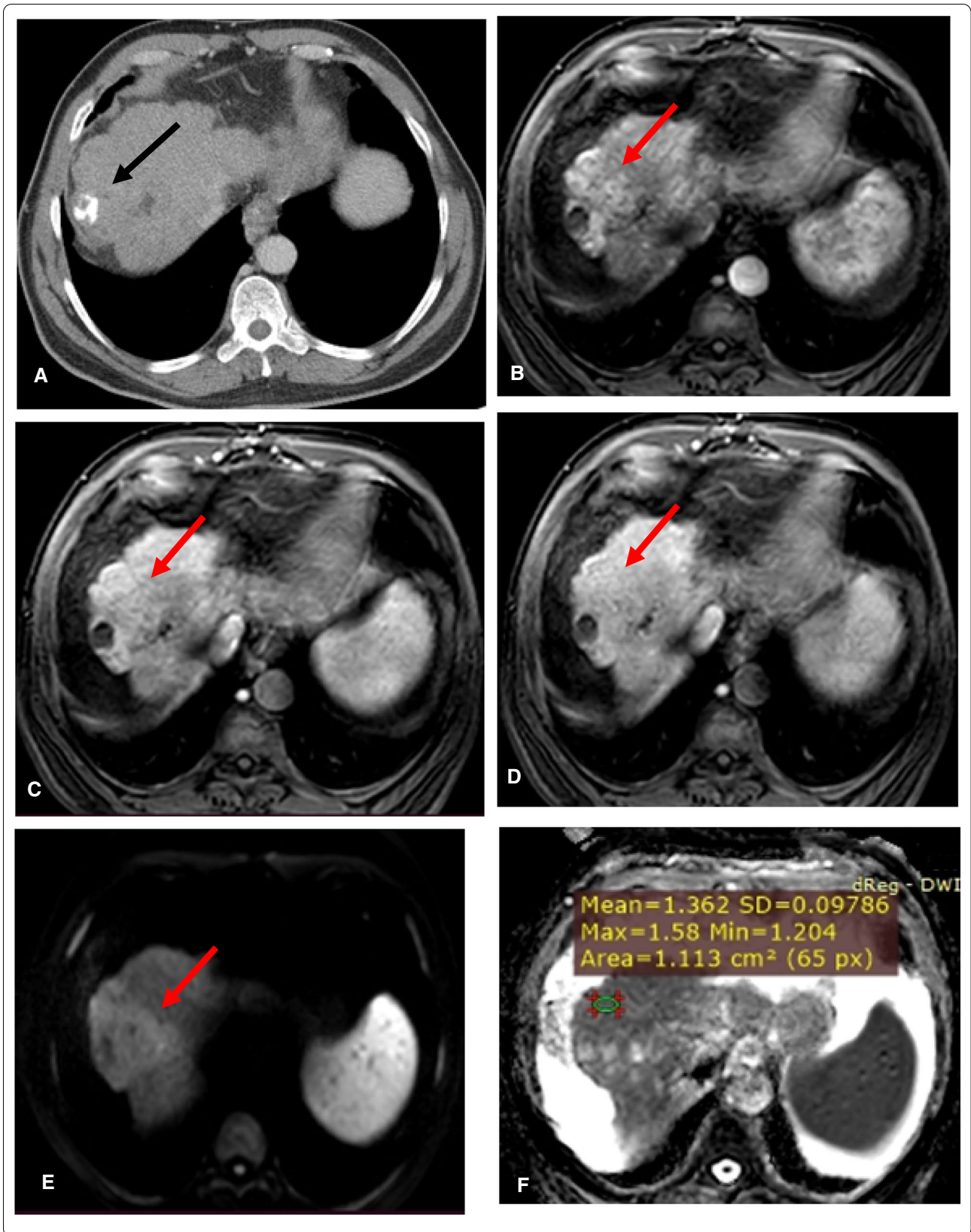
HCC is one of the most common primary hepatic tumors worldwide [1, 2]. The first line of HCC treatment is surgical resection and liver transplantation, yet few patients can be treated surgically, at the time of diagnosis. TACE is considered a palliative treatment for HCC and partial response after TACE therapy occurs in $15\text{--}55\%$ of the patients, so early assessment of the response to therapy is important for guiding further treatment [19].

CT was considered the first imaging tool for follow up the patient after TACE yet beam hardening artefact that occurs after TACE may hinder the proper evaluation of the residual/viable enhancing tumor by CT scans [4]. In contrast to CT scan, MRI signals are not degraded by lipiodol droplets; so, a residual or newly developed lesion are better to be detected by MRI study [3].

Dynamic contrast-enhanced cross-section images detect the change in the size of the residual tumor and the enhancement pattern of the lesion [1] while FDG PET/CT is a functional biomarker that detects mainly the metabolism of the lesion which reflects the presence of underlying viable tumoral tissue [20, 21], DWI gives information about the degree of tumor viability, whereas

(See figure on next page.)

Fig. 4 74 years old male patient underwent TACE. PET/CT uptake with no diffusion restriction in TR-LR viable lesion. **A** Axial CT venous phase showing focal peripheral lipiodol concentration (black arrow). **B–D** Arterial (**B**), venous (**C**) and delayed (**D**) DCE-MRI showing faint APHE with washout (red arrow) (TR-LR viable). **E, F** DWI (**E**) and ADC map (**F**) showing no diffusion restriction in the DWI with an iso-intense signal to the liver parenchyma in the ADC map. ADC of the lesion measures about $1.36 \times 10^{-3} \text{ mm}^2/\text{s}$ (above the cut off value of 1.32). **G–I** Fused PET/CT images showing mild peripheral increased FDG uptake achieving SUV max of 3.4 while the mean SUV of the liver parenchyma was 2.78 . (SUV ratio is 1.22)



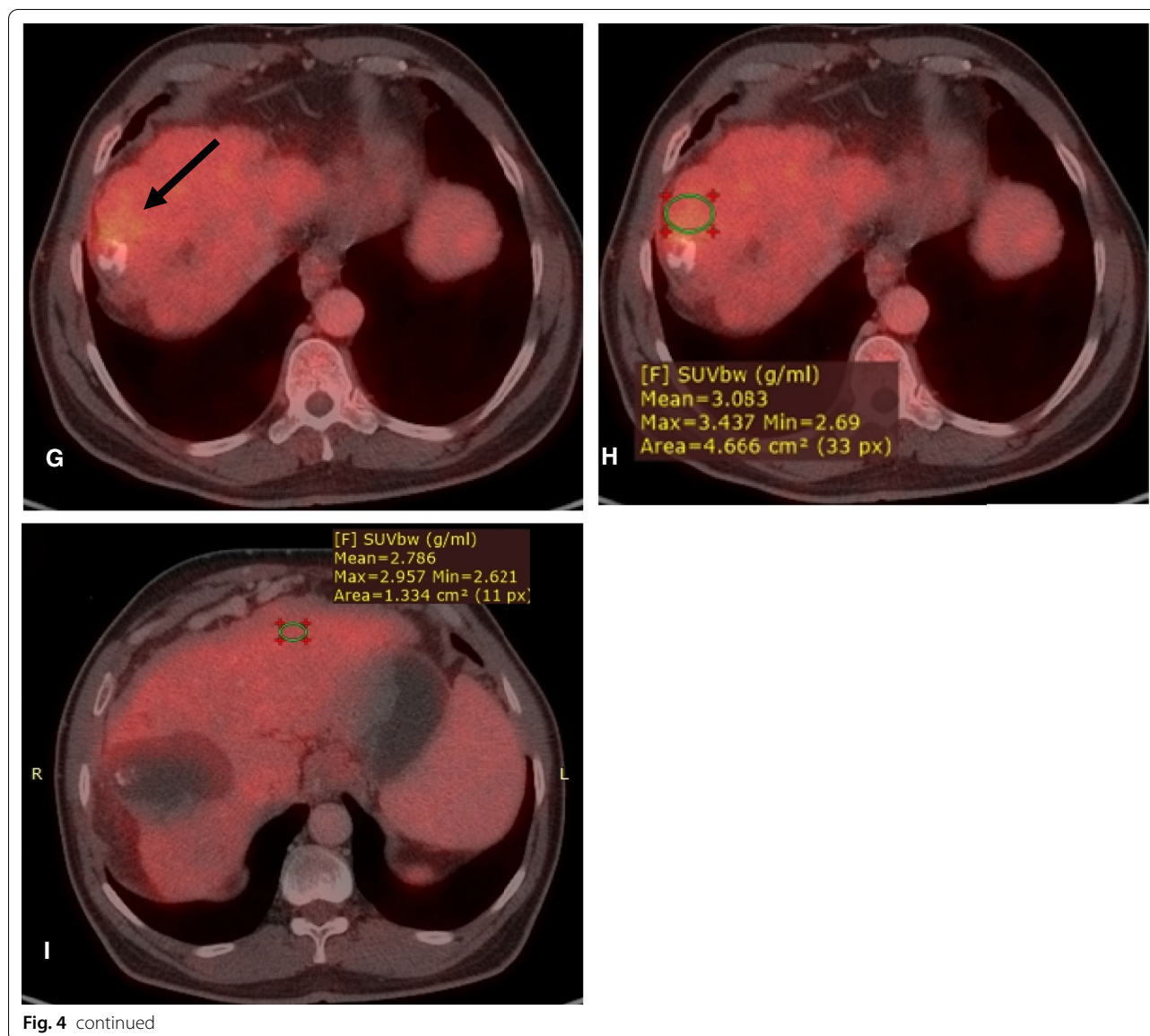


Fig. 4 continued

the necrotic tumors have increased water diffusibility and increased ADC values due to cell membrane damage, while the viable tumoral tissue shows diffusion restriction of the water and relatively low ADC values [22].

In this study, the well-embolized HCC lesion appeared visually as photopenic area in the FDG PET/CT images

while the residual viable tumoral tissue showed variable FDG uptake in the fused images, the sensitivity, specificity, and accuracy of qualitative FDG PET/CT for detection of residual viable tumoral tissue were 81.5%, 75%, and 80% respectively, similar results were also noted by and Kim et al. [11] and Song et al. [23], who reported sensitivity of 87.5%

(See figure on next page.)

Fig. 5 57 years old male patient underwent TACE. Diffusion restriction in TR-LR viable lesion with no PET/CT uptake. **A–D** Pre-contrast (**A**), arterial (**B**), venous (**C**) and delayed (**D**) phases of triphasic CT showing a large exophytic lesion with heterogeneous lipiodol concentration. The anterior portion of the lesion shows residual viable enhancement in the arterial phase with enhancing artery (red arrow) and washout of the contrast in the venous and delayed phases. **E–G** Fused PET/CT images showed mild increased FDG uptake with SUV ratio measuring 1.06 (tumor SUV max is 2.66 and the liver SUV mean is 2.75 (SUV ratio is 0.96). **H, I** DWI (**H**) and ADC (**I**) show restricted diffusion in the viable lesion with ADC value measuring $0.89 \times 10^{-3} \text{ mm}^2/\text{s}$

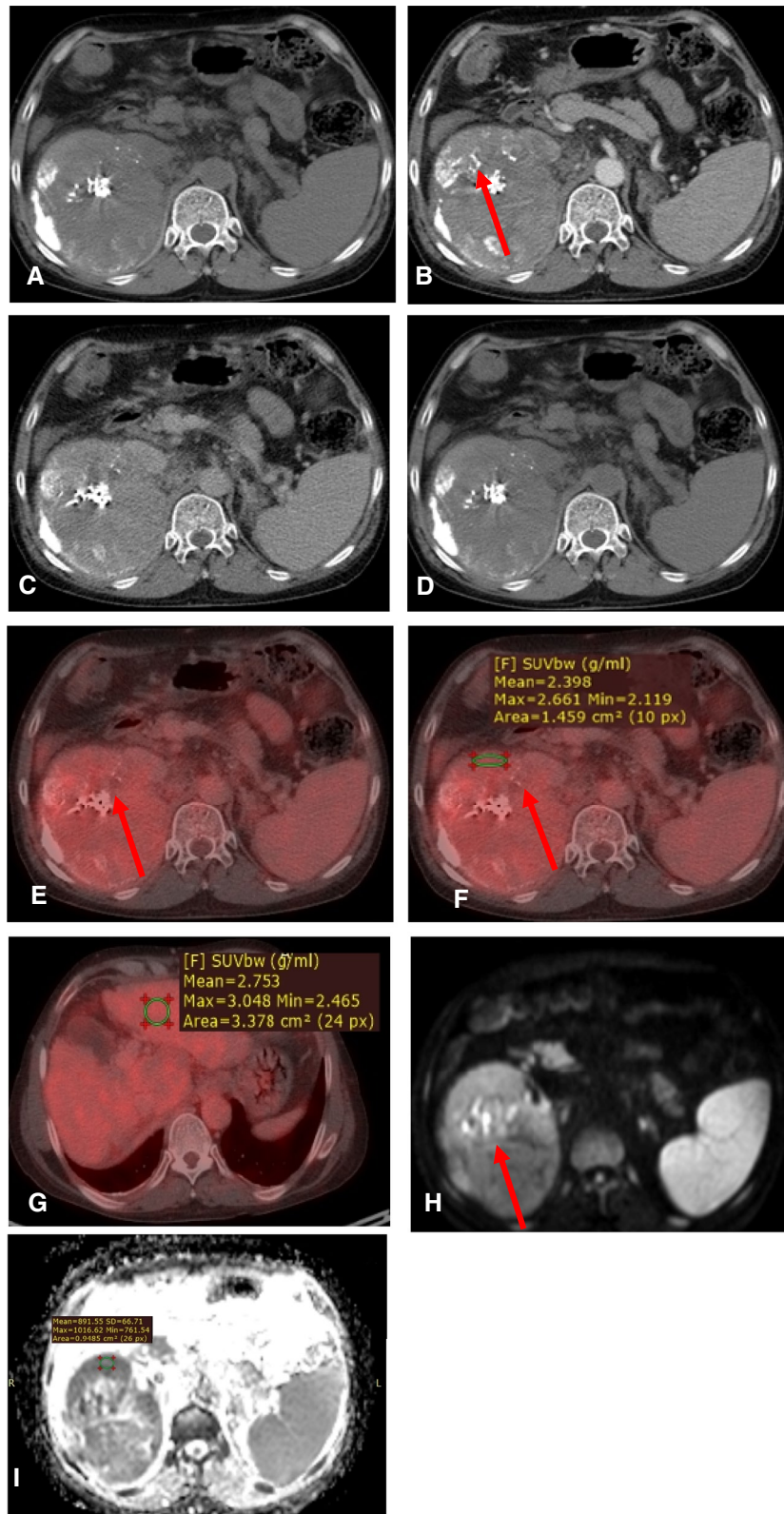


Fig. 5 (See legend on previous page.)

and 89.3%, specificity of 71.4% and 65.7% and accuracy of 80% and 80.2% respectively. The well-differentiated HCC didn't retain much glucose and appear in FDG PET/CT as the normal hepatocytes while the poorly differentiated HCCs tend to show a high activity of the glycolytic enzyme and hence in the detectability by FDG PET/CT [23].

The mean values of the residual SUV_{max} and the SUV ratio (residual tumor SUV_{max} /liver SUV_{mean} ratio) were higher than the values seen in the well-ablated lesion. The FDG uptake is affected by underlying liver cirrhosis which is noted in many of HCC patients and many studies have revealed that the SUV ratio is a more important parameter than the tumor SUV [10, 24], as it reflects the variation in glucose metabolism in both the tumor and the liver than the tumor's SUV does alone [24].

The quantitative assessment of SUV ratio revealed that the optimal cut off value for discrimination between the residual HCC and the well ablated HCC was 1.09 with sensitivity and specificity of 88.9% and 87.5% respectively, near similar cut off value was noted in Hetta et al. [14], who revealed that the optimal cut off value was 1, another study was done by Song et al. [24], revealed a higher cut off value of 1.65, the more aggressive residual tumor growth in their study may explain the higher ratio of this study. The SUV ratio was considered as an independent predictor for HCC response after TACE [24]. An advantage of the FDG PET/CT is the detection of extrahepatic metastases, in the current study, extrahepatic metastases were detected by FDG PET/CT in three patients, one was in the abdominal LNs which was also seen in the dynamic cross-section imaging, and the other two metastatic lesions were seen in chest and brain which were missed by the dynamic cross-section imaging.

In the current study, the sensitivity and specificity of the qualitative DWI for the detection of residual viable HCC after TACE were 77.8% and 75% respectively, a similar result was also noted in Ebeed et al. [3] study who revealed 82.3% sensitivity and 73.9% specificity. Saleh et al. [1] revealed different diagnostic values with a lower sensitivity of 52.6% and higher specificity of 90.5%, their study incorporated LR-TR non-evaluable HCC which was excluded in this study.

The sensitivity of quantitative ADC value was higher than the DWI for the detection of residual HCC, with a sensitivity and specificity of 81.5% and 75% respectively

at ADC cut off value of $1.32 \times 10^{-3} \text{ mm}^2/\text{s}$, a higher cut off value was reported by Ebeed et al. [3] who revealed a sensitivity of 76.5% and specificity of 65.2% at a cut off value of $1.38 \times 10^{-3} \text{ mm}^2/\text{s}$.

According to logistic regression analysis, the current study revealed that the ADC value was the most significant functional imaging variable for predicting viable HCC, with the optimal ADC value for predicting viable HCC being $1.35 \times 10^{-3} \text{ mm}^2/\text{s}$ with 88.6% accuracy. A similar result was reported by Saleh et al. [1], who revealed an accuracy of 82.5% at a cut off value of $1.35 \times 10^{-3} \text{ mm}^2/\text{s}$.

The LI-RAS v2018 has involved major and minor criteria for categorization of the non-treated hepatic focal lesion, and the DWI was considered one of its minor features, yet LI-RADS treatment response depends only upon the enhancement pattern of the treated HCC, and it didn't incorporate the DWI, ADC or the FDG PET/CT. In our study the accuracy of ADC and SUV ratio were comparable, and further studies may reveal the added value of ADC and PET/CT for the detection of the residual HCC after TACE. The standardized reporting method must be a dynamic process, subjected to clinical and radiological feedback and data validation, for further evaluation and development [25, 26], both DWI and FDG PET/CT gained the advantage of avoiding contrast administration, which may be a major problem in patients suffering from renal impairment.

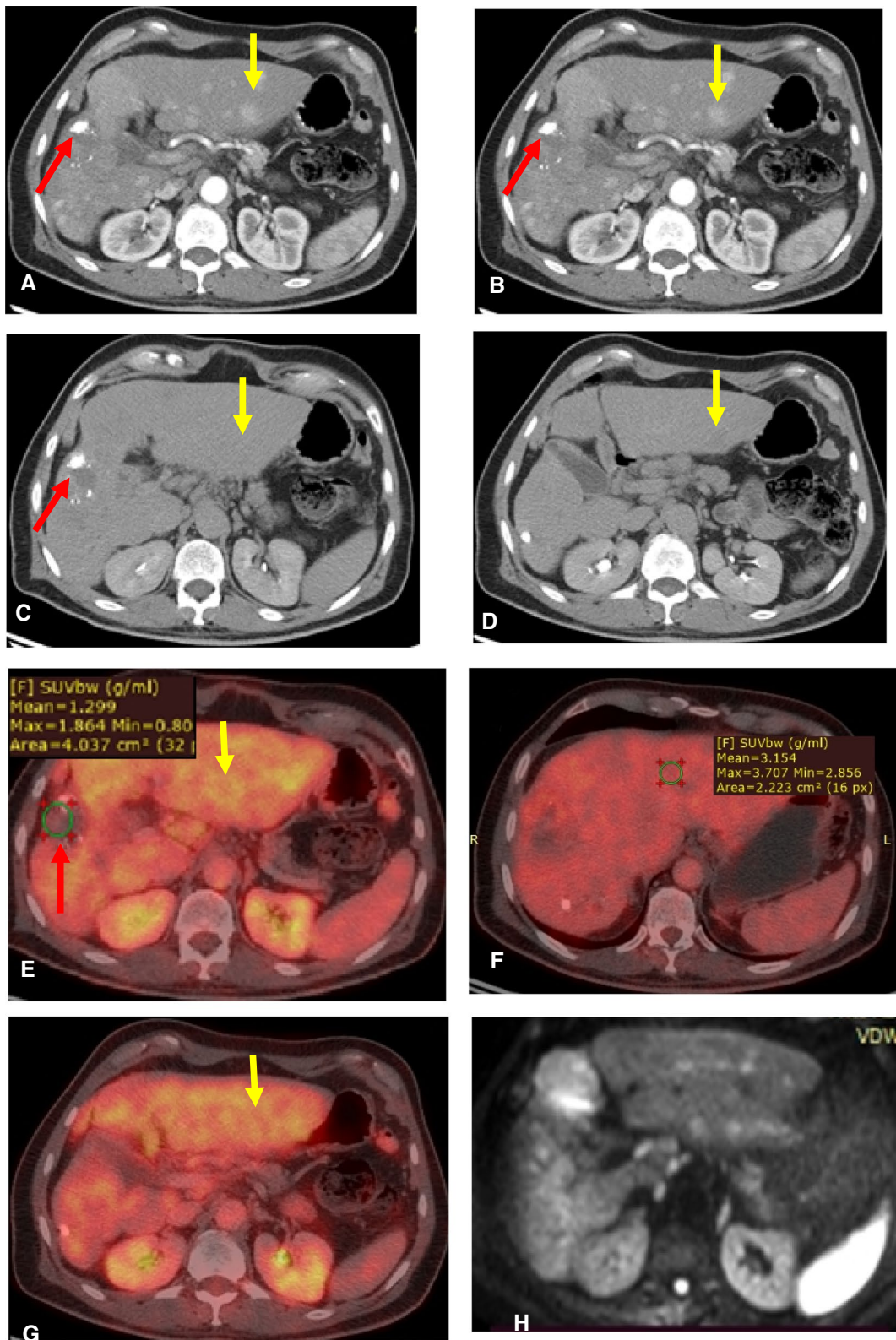
To summarize the implication of various functional imaging modalities and based upon the logistic regression analysis, we proposed that if a local residual or recurrent tumoral tissue is suspected following TACE, the imaging modality of choice will be an MRI study with anatomical, functional images such as DWIs and ADC, and dynamic contrast study. PET/CT, on the other hand, will be the imaging modality of choice if alpha-fetoprotein is substantially increased with probable metastatic deposits since it can evaluate the hepatic focal lesion and precisely locate any distant metastatic deposits.

Limitation

Some limitations were met in this study. First, the bias related to this retrospective study which may be related to the patient selection by the referring physician to

(See figure on next page.)

Fig. 6 60 years old male patient underwent TACE. TR-LR nonviable lesion with no PET/CT uptake yet with diffusion restriction, and PET uptake in de novo HCCs and metastatic mediastinal LNs. **A–D** Arterial (**A, B**), and delayed (**C, D**) triphasic CT showing partial lipiodol retention (red arrow) in a nonviable HCC, and multiple de novo HCCs, the largest (yellow arrow) shows APHE and washout. **E–G** PET/CT study shows no uptake in the ablated HCC with SUV_{max} measuring 1.86 (**E**), mean SUV of normal hepatic parenchyma is 3.15 (**F**) (SUV ratio is 0.59), focal uptake is seen in the de novo HCC (**G**). **H, I** DWI and ADC map shows restricted diffusion in the ablated HCC with ADC value measuring $1.18 \times 10^{-3} \text{ mm}^2/\text{s}$. **J, K** DWI and ADC map shows restriction diffusion of the de novo lesion with an ADC value of $0.937 \times 10^{-3} \text{ mm}^2/\text{s}$. **L, M** PET/CT shows multiple metabolically active mediastinal lymphadenopathies (extra-hepatic metastases) with SUV_{max} measuring about 5 (green circle)



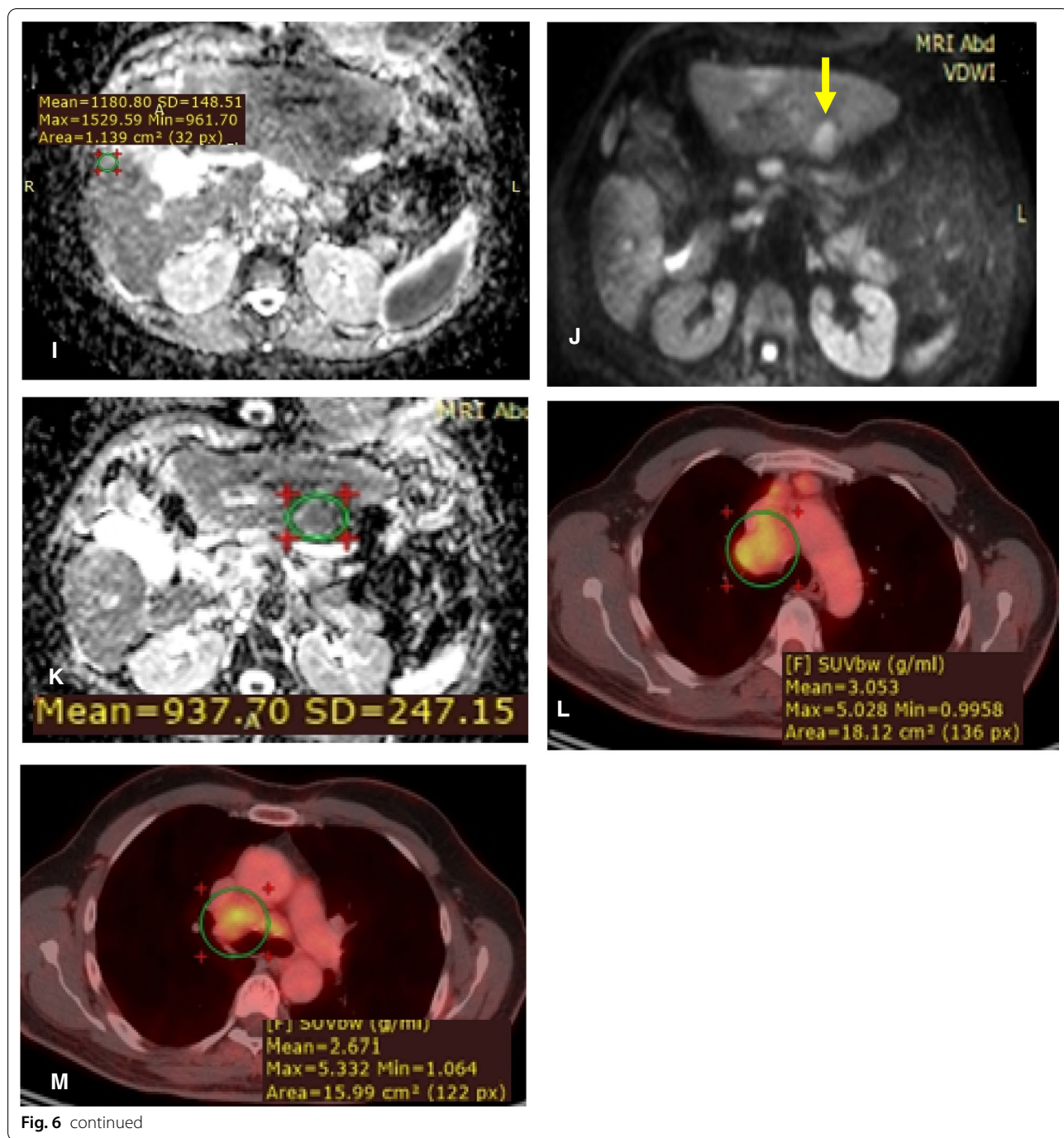


Fig. 6 continued

undergone FDG PET/CT. The exclusion of LR-TR equivocally viable in our study may reduce this bias. Second, the relatively low number of involved patients, the cost of FDG PET/CT may partly explain this issue, many studies also involved comparable patient numbers [1, 3, 11]. Finally, the histopathological results were not available for all patients, we included only the LI-TR viable and LR-TR nonviable lesion in our study.

Conclusions

The FDG PET/CT and DWI with ADC map showed comparable diagnostic performance for detection of post-TACE residual HCC and it can substitute the dynamic cross-section studies in many situations when the contrast administration is contraindicated. Another advantage of FDG PET/CT is its ability to detect extrahepatic metastases in a single examination.

Table 4 Logistic regression for each variable for predicting post-TACE viable HCC

Variable	Odd ratio	95% CI	p value	B
DWI	10.5	1.668–66.087	0.012*	2.351
PET	13.2	2.031–85.805	0.007*	2.580
ADC	0.000067	8.402–0.536	0.036*	– 9.609
SUV ratio	44,219.9	4.538–4,308,961	0.022*	10.697

95% CI 95% confidence interval

*Significant

Table 5 Multinomial logistic regression model including all variables (using enter method) for predicting post-TACE viable HCC

	Odd ratio	95% CI	p value	B
Intercept	194,254,144	–	0.435	19.085
DWI	0.031	0.000002–579.1	0.489	– 3.470
PET	0.655	0.00016–2671.2	0.921	– 0.423
ADC	2.825	7.328–108,900.2	0.217	– 19.685
SUV ratio	2893.1	0.009–882,887,891.1	0.216	7.970

95% CI 95% confidence interval

*Significant

Table 6 Logistic regression for the best model (ADC) for predicting post-TACE viable HCC

	Odd ratio	95% CI	p value	B
Intercept	7,139,999	–	0.025	13.479
ADC	0.000067	8.402–0.536	0.036	– 9.609

95% CI 95% confidence interval

*Significant

Abbreviations

HCC: Hepatocellular carcinoma; TACE: Transcatheter arterial chemoembolization; FDG: ¹⁸F-2-Fluoro-2-deoxyglucose; PET/CT: Positron emission tomography–computed tomography; CECT: Contrast-enhanced computerized tomography; DCE-MRI: Dynamic contrast-enhanced magnetic resonance imaging; LI-RADS: Liver imaging reporting and data system; DWI: Diffusion-weighted image; ADC: Apparent diffusion coefficient; SUV: Standardized uptake value; TSE: Turbo spin-echo; EPI: Echo-planar imaging; THRIVE: T1-weighted high-resolution isotropic volume examination; AASLD: American Association for the Study of Liver Diseases; ROC: Receiver operator characteristic; SD: Standard deviation; THAD: Transient hepatic attenuation differences; TP: True positive; TN: True negative; FP: False positive; FN: False negative.

Acknowledgements

Not applicable.

Authors' contributions

AS: results and statistics, revising the manuscript. AS: idea of the research, manuscript writing. NM: idea of the research, collecting cases, manuscript writing. All authors read and approved the final manuscript.

Funding

No funds, sponsorship or financial support to be disclosed.

Availability of data and material

The datasets used and/or analyzed during the current study are available from the corresponding author on reasonable request.

Declarations**Ethics approval and consent to participate**

This study was approved by the Research Ethics Committee of the Faculty of Medicine at Ain Shams University in Egypt (FWA 000017585); Reference Number of approval: R46/2020. The requirement for written consent was waived in this retrospective study.

Consent for publication

Not applicable.

Competing interests

The authors declare that they have no competing interest.

Received: 14 February 2021 Accepted: 22 August 2021

Published online: 31 August 2021

References

- Saleh TY, Bahig S, Shebrya N et al (2019) Value of dynamic and DWI MRI in evaluation of HCC viability after TACE via LI-RADS v2018 diagnostic algorithm. *Egypt J Radiol Nucl Med* 50:113. <https://doi.org/10.1186/s43055-019-0120-x>
- Cho K, Choi N, Shin M et al (2017) Clinical usefulness of FDG-PET in patients with hepatocellular carcinoma undergoing surgical resection. *Ann Hepatobiliary Pancreat Surg* 21:194–198
- Ebeed A, Romeih M, Refat M et al (2017) Role of dynamic contrast-enhanced and diffusion weighted MRI in evaluation of hepatocellular carcinoma after chemoembolization. *Egypt J Radiol Nucl Med* 48:807–815
- Kim H, Kim J, Shin Y et al (2010) Evaluation of metabolic characteristics and viability of lipiodolized hepatocellular carcinomas using ¹⁸F-FDG PET/CT. *J Nucl Med* 51:1849–1856
- Sergio A, Cristofori C, Cardin R et al (2008) Transcatheter arterial chemoembolization (TACE) in hepatocellular carcinoma (HCC): the role of angiogenesis and invasiveness. *Am J Gastroenterol* 103:914–921
- Lee JK, Chung YH, Song BC et al (2002) Recurrences of hepatocellular carcinoma following initial remission by transcatheter arterial chemoembolization. *J Gastroenterol Hepatol* 17:52–88
- Raoul JL, Forner A, Bolondi L et al (2019) Updated use of TACE for hepatocellular carcinoma treatment: how and when to use it based on clinical evidence. *Cancer Treat Rev* 72:28–36
- Van Beers BE, Daire JC, Garteiser P (2015) Erratum to "New imaging techniques for liver diseases". *J Hepatol*; 62: 690–700. *J Hepatol* 63(3):774
- Elsayes KM, Hooker JC, Agrons MM et al (2017) 2017 Version of LI-RADS for CT and MR imaging: an update. *Radiographics* 37(7):1994–2017. <https://doi.org/10.1148/rg.2017170098>
- Seo S, Hatano E, Higashi T et al (2007) Fluorine-18 fluorodeoxyglucose positron emission tomography predicts tumor differentiation, P-glycoprotein expression, and outcome after resection in hepatocellular carcinoma. *Clin Cancer Res* 13:427–433
- Kim SH, Won KS, Choi BW et al (2012) Usefulness of F-18 FDG PET/CT in the evaluation of early treatment response after interventional therapy for hepatocellular carcinoma. *Nucl Med Mol Imaging* 46:102–110
- Hayakawa N, Nakamoto Y, Nakatani K et al (2014) Clinical utility and limitations of FDG PET in detecting recurrent hepatocellular carcinoma in postoperative patients. *Int J Clin Oncol* 19(6):1020–1028. <https://doi.org/10.1007/s10147-013-0653-3>
- Lin C-Y, Chen J-H, Liang J-A et al (2011) ¹⁸F-FDG PET or PET/CT for detecting extrahepatic metastases or recurrent hepatocellular carcinoma: a systematic review and meta-analysis. *Eur J Radiol* 81:2417–2422
- Hetta WM, Atyia HR (2020) Role of PET CT in comparison to triphasic CT in early follow-up of hepatocellular carcinoma after transarterial chemoembolization. *Egypt J Radiol Nucl Med* 51:33. <https://doi.org/10.1186/s43055-020-0150-4>

15. ElSaid NAE, Kaddah RO et al (2016) Subtraction MRI versus diffusion weighted imaging: which is more accurate in assessment of hepatocellular carcinoma after trans arterial chemoembolization (TACE)? *Egypt J Radiol Nucl Med* 47(4):1251–1264
16. Buijs M, Vossen JA, Hong K et al (2008) Chemoembolization of hepatic metastases from ocular melanoma assessment of response with contrast-enhanced and diffusion weighted MRI. *AJR Am J Roentgenol* 191(1):285–289
17. American College of Radiology. CT/MRI LI-RADS v2018 core. Liver Imaging Reporting and Data System. <https://www.acr.org/-/media/ACR/Files/RADS/LI-RADS/LI-RADS-2018-Core.pdf>
18. Marrero JA, Kulik LM, Sirlin CB et al (2018) Diagnosis, staging, and management of hepatocellular carcinoma: 2018 practice guidance by the American Association for the Study of Liver Diseases. *Hepatology* 68(2):723–750. <https://doi.org/10.1002/hep.29913>
19. Ma W, Jia J, Wang S et al (2014) The prognostic value of ¹⁸F-FDG PET/CT for hepatocellular carcinoma treated with transarterial chemoembolization (TACE). *Theranostics* 4(7):736–744
20. Guindalini F, Botelho M, Harmath C et al (2013) Assessment of liver tumor response to therapy: role of quantitative imaging. *Radiographics* 33:1781–1800
21. Wong SC, Ngai WT, Choi FPT (2017) Update on positron emission tomography for hepatocellular carcinoma. *Hong Kong J Radiol* 20:192–204
22. Santhi M, Janio S (2010) Magnetic resonance imaging: review of imaging techniques and overview of liver imaging. *World J Radiol* 2(8):309–322
23. Song HJ, Cheng JY, Hu LS et al (2015) Value of ¹⁸F-FDG PET/CT in detecting viable tumour and predicting prognosis of hepatocellular carcinoma after TACE. *Clin Radiol* 70:128–137
24. Song MJ, Bae SH, Lee SW et al (2013) (18)F-Fluorodeoxyglucose PET/CT predicts tumour progression after transarterial chemoembolization in hepatocellular carcinoma. *Eur J Nucl Med Mol Imaging* 40:865–873
25. Abdelrahman AS, Ashour MMM, Abdelaziz TT (2020) Predictive value of neck imaging reporting and data system (NIRADS) in CECT/CEMRI of laryngeal and oral cavity squamous cell carcinoma. *Egypt J Radiol Nucl Med* 51:241
26. Abdelaziz TT, Abdel Razk AAK, Ashour MMM et al (2020) Interreader reproducibility of the neck imaging reporting and data system (NI-RADS) lexicon for the detection of residual/recurrent disease in treated head and neck squamous cell carcinoma (HNSCC). *Cancer Imaging* 20:61

Publisher's Note

Springer Nature remains neutral with regard to jurisdictional claims in published maps and institutional affiliations.

Submit your manuscript to a SpringerOpen[®] journal and benefit from:

- Convenient online submission
- Rigorous peer review
- Open access: articles freely available online
- High visibility within the field
- Retaining the copyright to your article

Submit your next manuscript at ► [springeropen.com](https://www.springeropen.com)
